

MITIGATING WATERBORNE HEALTH RISKS THROUGH MALACHITE GREEN BIOSORPTION USING TEA WASTE-DERIVED MATERIAL

Northaqifah Hasna Mohamed Khir^{1,2}, Nur Fatien Muhamad Salleh², Mohd Shahrul Nizam Salleh^{3*}, Abdul Mu'iz A Zuhari³, Amirul Ammar Rosmini³, Nur Ainin Rabithah Mohd Zolkifli³

¹Faculty of Applied Sciences, Universiti Teknologi MARA, Terengganu Branch, Bukit Besi Campus, Dungun 23200, Terengganu, Malaysia

²School of Health Sciences, Universiti Sains Malaysia, Health Campus, Kubang Kerian 16150, Kelantan, Malaysia

³Faculty of Chemical Engineering, Universiti Teknologi MARA, Terengganu Branch, Bukit Besi Campus, Dungun 23200, Terengganu, Malaysia

Corresponding Author:

*) shahrulnizam@uitm.edu.my

Article Info

Submitted : 29 March 2025
In reviewed : 14 May 2025
Accepted : 10 June 2025
Available Online : 31 July 2025

Keywords : Biosorption, Iron modification, Malachite green, Tea waste

Published by Faculty of Public Health
Universitas Airlangga

Abstract

Introduction: Malachite green (MG) is a synthetic dye extensively used in the textile and aquaculture industries, known for its toxicity, bioaccumulation potential, and environmental persistence which poses significant public health risks. This study investigates the biosorption performance of raw tea waste (RTW) and iron-coated tea waste (FeTW) for MG removal as a low-cost and sustainable water treatment solution. **Methods:** A laboratory-based batch biosorption experiment was conducted under parameters of contact time, biosorbent dosage and initial MG concentration using biosorbents of RTW and FeTW. The MG removal efficiency was quantified using a Hach DR900 spectrophotometer. Functional group characterization was conducted via FTIR spectroscopy, and adsorption behaviours were analysed using Langmuir and Freundlich isotherm models. **Results and Discussion:** FeTW demonstrated superior performance compared to RTW under all conditions. A maximum removal efficiency of 68.54% was achieved using 0.5g of FeTW at an initial MG concentration of 25mg/L within 60 minutes. FTIR analysis revealed enhanced hydroxyl group intensity at 3360cm^{-1} and the appearance of Fe-O bonds at 560cm^{-1} , confirming successful surface modification. The Langmuir isotherm model best described the biosorption behavior with R^2 of 0.9901 and maximum biosorption capacity (qm) of 3.12mg/g. The low separation factor (RL) value of 0.00025 indicated highly favorable biosorption. **Conclusion:** These findings demonstrate the potential of FeTW as an eco-friendly biosorbent to reduce human exposure to MG, a known carcinogenic contaminant in water systems. Iron modification significantly enhances the biosorption capacity of tea waste for MG removal and contributes to safer water quality and reduced public health risks.

INTRODUCTION

Water contamination by hazardous pollutants remains one of the most critical global challenges, significantly impacting public health and environmental sustainability. Among these pollutants, synthetic dyes specifically MG are particularly alarming due to their extensive use in industries like textile manufacturing, aquaculture, and paper production (1,2). MG is a cationic dye with high toxicity, mutagenicity, and carcinogenic potential, posing significant dangers to aquatic ecosystems and human health. Prolonged exposure to

MG has been connected to liver damage, respiratory distress, and possible carcinogenesis, highlighting the critical need for its effective removal from wastewater (3,4). Despite regulatory bans in many countries, MG continues to be detected in aquaculture products and water bodies, particularly in Southeast Asia. Recent analyses in Malaysia found MG and its metabolite, leucomalachite green (LMG), in commonly consumed fish species, with concentrations ranging from 0.53 to 4.10 µg/kg, exceeding recommended safety thresholds in some cases. A broader review also reported MG residues

Cite this as :

Khair NHM, Salleh NFM, Salleh MSN, Zuhari AMA, Rosmini AA, Zolkifli NARM. Mitigating Waterborne Health Risk Through Malachite Green Biosorption Using Tea Waste-Derived Material. *Jurnal Kesehatan Lingkungan*. 2025;17(3):201-209. <https://doi.org/10.20473/jkl.v17i3.2025.201-209>



This is an open-access article distributed under
[CC BY NC-SA 4.0 license](https://creativecommons.org/licenses/by-nc-sa/4.0/).

©2025 Jurnal Kesehatan Lingkungan all right reserved.

in fish from multiple countries, reaching levels as high as 146 µg/kg, posing significant carcinogenic and genotoxic risks to consumers (5,6). These findings emphasise the continuous overuse of MG and the crucial need for low-cost, effective removal techniques to preserve the environment and public health.

Traditional dye removal methods, such as chemical precipitation, coagulation, and advanced oxidation processes, face numerous challenges, including high operational costs, secondary pollution, and inefficiencies at low concentrations. In contrast, biosorption has emerged as a preferred alternative due to its simplicity, high removal efficiency, and cost-effectiveness (7-11). However, the performance of biosorption largely depends on the choice of biosorbent. Recent advancements emphasize the use of agricultural and industrial waste materials as sustainable biosorbents, aligning with the principles of waste valorization and the circular economy (12-20). Among these, tea waste as a globally abundant by-product of tea production has shown promising potential owing to its natural abundance, biodegradability, and inherent biosorption properties.

Despite these advantages, RTW exhibits limited biosorption capacity due to insufficient functional groups and structural characteristics essential for effective dye removal. To overcome these limitations, modifications such as coating tea waste with magnetic materials like iron have been explored (21). Magnetic modification enhances biosorption performance by introducing active binding sites, improving surface functionality, and adding magnetic properties that facilitate recovery and reuse of the biosorbent, addressing a significant drawback of conventional biosorption techniques.

This research examines the efficacy of FeTW as an innovative, sustainable, and economical biosorbent for the removal of malachite green from water solutions. This study assesses the biosorption capacity and isotherms of Langmuir and Freundlich, while comparing the performance of RTW and FeTW. The study posits that iron coating markedly improves biosorption efficiency by augmenting active binding sites and incorporating magnetic properties, thereby presenting a viable approach for wastewater treatment.

This study reinforces the United Nations' Sustainable Development Goals (SDGs), especially SDG 6 for clean water and sanitation, SDG 12 for responsible consumption and production, and SDG 14 for life below water (22). The study addresses water pollution and encourages the reuse of industrial waste by offering a sustainable approach to wastewater treatment. This helps safeguard water resources and ecosystems around the world. Also, making a low-cost, effective

biosorbent helps everyone have fair access to clean water, which is a key part of sustainable development. By utilising waste-derived materials, the study emphasises the need of incorporating environmental sustainability into inventive solutions to pressing global concerns, while also providing practical insights into dealing with waterborne health threats.

METHODS

The tea wastes of a Malaysian tea brand called BOH Tea were obtained from a cafeteria, located at the Universiti Teknologi MARA (UiTM) Terengganu Branch Bukit Besi Campus, Terengganu, Malaysia. The research encompassed two variations of tea waste biosorbents: uncoated (RTW) and magnetic iron coated (FeTW). The experimental design consisted of batch biosorption experiments conducted in a controlled laboratory setting. The performance of RTW and FeTW was compared under various conditions, including contact times (15, 30, 45, 60, 75, 90, 105, and 120 minutes), initial concentration (10, 25, 50, 75, 100 mg/L) and biosorbent dosages (0.05, 0.1, 0.2, 0.3, 0.4, 0.5 g) in controlled temperature. A handheld colorimeter by Hach DR900 was used at a wavelength of 610 nm for the quantification of MG in the aqueous solutions. FTIR spectroscopy was used for the characterization. Data analysis was conducted using IBM SPSS Statistics 26, employing isotherm modelling to evaluate and compare the biosorption performance of RTW and Fe-TW. The isotherm models provided critical insights into the biosorption capacity and surface interactions of Fe-TW.

Chemicals

Malachite green, iron(III) nitrate nonahydrate, sodium hydroxide (NaOH), and hydrochloric acid (HCl) were obtained from Merck. Reagents of all the elements are of analytical purity and were used as it is except that; pH of solution was adjusted to by using 1M HCl and 1M NaOH. The solvents utilized were laboratory-made distilled water.

Preparation of biosorbents

For the preparation of RTW biosorbent, a total of 15g TW was washed with hot distilled water at 80°C and then dried at 110°C for 3 hours in a hot oven. The washing and drying process was conducted to eliminate impurities and remove color. The dried material was then sieved and stored in an airtight container for further use. The researcher thoroughly washed the obtained TW to remove any adhering dirt before drying in an oven at 60°C. The drying process was carried out until a constant weight was achieved. The dried TW were finely ground

and stored in airtight containers for further use (23).

Introduction of Fe as magnetic compound into TW began by activating RTW with 1.0 M HCl for 3 hours using a magnetic stirrer. The biosorbent was later washed several times with deionized water and dried at 110°C for 3 hours. The mixture was then filtered, and the solid residue was rinsed several times with distilled water to eliminate any remaining acid. The residue was then dried in an oven at 60°C until a constant weight was achieved. Then, 10 g of dried residue was stirred in distilled water at 40 °C for 10 minutes. At the same time, 5% (w/v) of Iron (II) Nitrate will be added into distilled water forming homogeneous mixture.

Characterization of biosorbents

The chemical characterization for both RTW and FeTW biosorbents was performed utilizing the KBr pellet technique, scanning from 400 to 4000 cm⁻¹ on the FTIR Bruker Tensor 27 Spectrometer. The FTIR spectra of both biosorbents were recorded and compared to identify changes in functional groups induced by acid treatment.

Batch biosorption study

A batch biosorption system was studied to assess the influence parameters of contact time at 15-minutes interval (15, 30, 45, 60, 75, 90, 105, and 120 minutes), biosorbent dosages (0.05, 0.1, 0.2, 0.3, 0.4, 0.5 g) and initial concentration (10, 25, 50, 75, 40, 100 mg/L) to investigate the efficacy of RTW and FeTW towards MG biosorption. 0.1 g of RTW and FeTW were added in two different 250 mL beakers containing 100 mL of a 25 mg/L MG solution. The solution was then stirred at 30°C using a magnetic stirrer before being collected in falcon tubes. Handheld colorimeter by Hach DR900 was used at a wavelength of 610 nm to determine the concentrations of MG before and after biosorption. Blank experiments were conducted to ensure the accuracy and precision of the measurements. For all the parameters, the process was replicated three times.

Biosorption Calculation and Isotherm Modelling

The removal percentage (%), was calculated using the following Eq. 1 (24).

$$\% = \frac{C_0 - C_e}{C_0} \times 100 \quad (1)$$

where C_0 and C_e are the initial and equilibrium concentrations (mg/L)

Data analysis using IBM SPSS Statistics 26 applied Langmuir and Freundlich isotherms to evaluate biosorption capacity and equilibrium behavior. The linear form of the Langmuir and Freundlich isotherm are represented by Eq. 2 and 4. The Langmuir constant, K_L and Freundlich constant, K_F were determined from the linear plots using Eq. 2 and 3, respectively. Additionally, the R_L for the Langmuir isotherm was computed from

Eq. 4, while the heterogeneity factor, n for the Freundlich isotherm was obtained from the slope of the linear regression (24,25).

$$\frac{1}{q_e} = \frac{1}{q_m K_L C_e} + \frac{1}{q_m} \quad (2)$$

$$\ln q_e = \ln K_F + (1/n) \ln C_e \quad (3)$$

$$R_L = \frac{1}{1 + C_0 K_L + C_0 K_L W} \quad (4)$$

where q_m denotes the maximum biosorbent's monolayer capacity for the adsorbate (mg/g).

Manuscript Assistance

The composition of the preliminary literature review and discussion parts was facilitated by OpenAI's GPT-4 model. The AI was employed to provide succinct literature reviews and formulate initial talks based on experimental findings. The authors rigorously evaluated, revised, and enhanced the content produced by the AI model to guarantee scientific accuracy, coherence, and alignment with the study's results.

RESULTS

The biosorption efficiency of tea waste (RTW and FeTW) for MG removal was evaluated under varying parameters, including contact time, initial concentration and biosorbent dosage, utilizing Hach DR900 for the analysis. FTIR spectra for both biosorbents were compared to determine the functional groups present in tea waste and the contribution to biosorption behavior.

FTIR Analysis

FTIR spectra of RTW and FeTW are presented in Figure1. Both biosorbents exhibited a broad absorption band around 3360 cm⁻¹, corresponding to O–H stretching vibrations. Notably, FeTW displayed a broader and more intense O–H band, indicating an increase in hydrogen bonding following surface modification. Peaks near 2920 cm⁻¹ were attributed to C–H stretching vibrations of aliphatic groups. In the FeTW spectrum, a distinct peak was observed at approximately 1730 cm⁻¹, corresponding to C=O stretching. Bands around 1600cm⁻¹ were associated with aromatic C=C and asymmetric COO⁻ stretching, while the signal near 1400cm⁻¹ was assigned to CH bending and symmetric COO⁻ stretching. The region between 1050–1100 cm⁻¹ exhibited peaks related to C–O–C and C–O stretching vibrations, characteristic of polysaccharide structures (26,27). A new absorption band around 560 cm⁻¹, observed exclusively in FeTW, corresponds to Fe–O stretching, confirming the successful incorporation of iron species onto the tea waste surface (28).

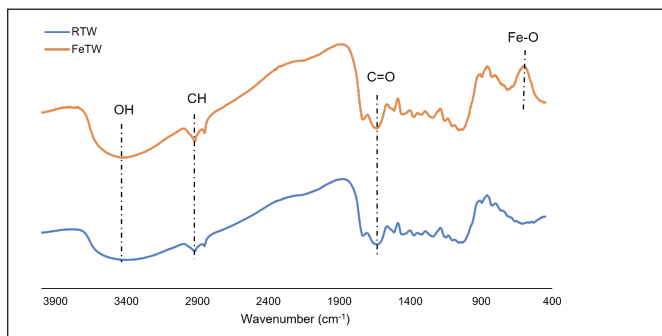


Figure 1. FTIR spectra of RTW and FeTW biosorbents

Batch Biosorption Findings

A comparative investigation was performed to assess the removal percentage of MG by RTW and FETW, which involved three influence parameters: contact time, initial concentration and biosorbent dosage.

Table 1 Biosorption Isotherm Parameters for MG Biosorption

Langmuir		Freundlich	
Parameters		Parameters	
q_m (g/mg)	3.12	K_F	0.1143
K_L (L/mg)	400.88	n	1.21
R^2	0.9901	R^2	0.9676
R_L	0.00025		

Effect of Contact time

The effect of contact time on the percentage removal of MG is illustrated in Figure 2, demonstrating the biosorption performance of RTW and FeTW at a biosorbent dosage of 0.5 g, an initial MG concentration of 10 mg/L, and pH 7.0. The removal efficiency of MG increased with contact time for both biosorbents, with a rapid biosorption phase observed within the first 30–45 minutes. FeTW exhibited a faster biosorption rate, reaching equilibrium at 60 minutes with a higher removal efficiency of 38.8%, whereas RTW took 90 minutes to reach equilibrium, achieving a lower removal efficiency of 34%. Higher percentage removal exhibited by FeTW indicates a higher biosorption capacity compared to RTW for MG removal.

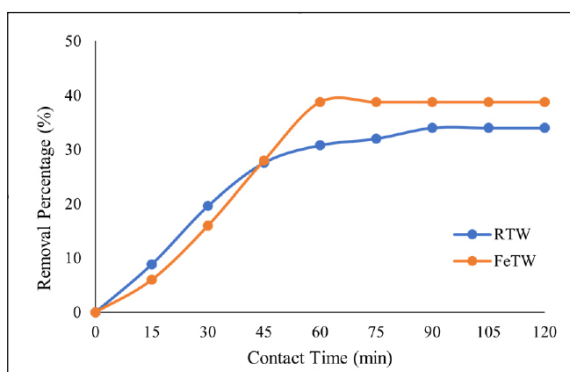


Figure 2 Effect of contact times (15 – 120 minutes) on percentage removal of MG using 0.5 g RTW and FeTW biosorbents with 25 mg L⁻¹ initial concentration at pH 5

Effect of biosorbent dosages

The effect of biosorbent dosage on MG removal efficiency is visualized in Figure 3. Specifically, the highest removal efficiency of 17.3% was achieved with 0.05 g of FeTW, which increases significantly to 38.8% at 0.1 g and 42.1% at 0.2 g respectively. A slight decline is observed at 0.3 g with 36.5% MG removal, followed by a notable increase at 0.4 g at 59.73% MG removal. The highest removal efficiency of 68.54% is achieved at 0.5 g, indicating the optimal biosorbent dosage. The trend suggests that increasing biosorbent dosage enhances removal efficiency up to a saturation point, beyond which excess biosorbent does not significantly improve MG biosorption.

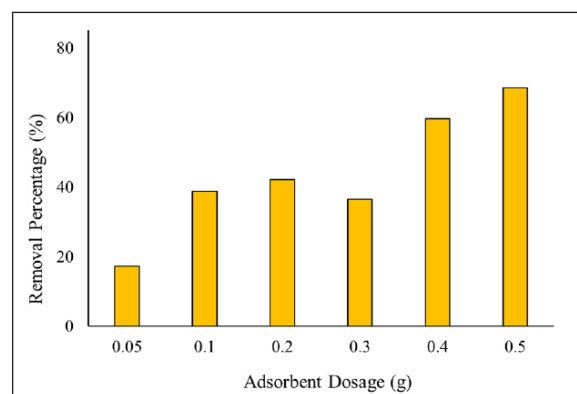


Figure 3 Effect of biosorbent dosage (0.05 - 0.5 g) on percentage removal of 25 mg L⁻¹ MG at pH 5 using FeTW biosorbents

Effect of Initial Concentration

The influence of initial concentration on the removal efficiency of MG ions is depicted in Figure 4, where 0.5 g Fe-TW biosorbent was used for biosorption. At 10 mg/L, the removal percentage is 59.6%, which increases significantly to 68.5% at 25 mg/L, indicating peak biosorption efficiency. As the concentration rises, removal efficiency declines, with 56.2% at 50 mg/L, 48.9% at 75 mg/L, and 39.0% at 100 mg/L. The trend suggests an optimal biosorption performance at 25 mg/L, with efficiency decreasing at higher concentrations due to saturation of active sites.

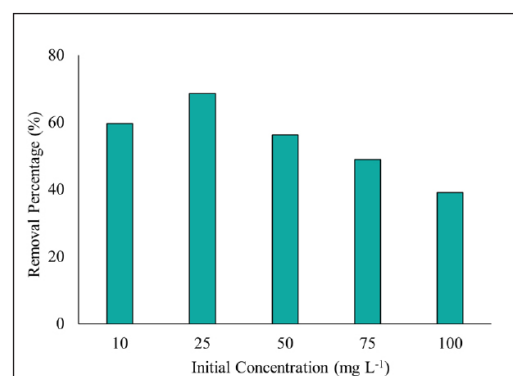


Figure 4 Effect of initial MG concentration (10 – 100 mg L⁻¹) at pH 5 on percentage removal using 0.5 g FeTW biosorbents

Statistical Analysis

The biosorption isotherm analysis demonstrates that the Langmuir, and Freundlich models all show strong correlations, as illustrated in Figure 5. The Langmuir model as in Figure 5A yielded a high linear correlation of $R^2 = 0.9901$, with the calculated Langmuir constants being q_m of 3.12 mg/g and K_L of 400.88 L/mg, obtained from the slope and intercept of the linearized plot of $1/C$ versus q_e . This suggests a monolayer biosorption process on a homogeneous surface. Meanwhile, the

dimensionless separation factor, R_L calculated was 0.00025, indicating highly favorable biosorption (29,30).

The Freundlich model also showed a good fit with $R^2 = 0.9676$, indicating biosorption on a heterogeneous surface. The linear equation yielded a Freundlich constant $n \approx 1.21$, signifying favorable biosorption conditions (31,32). These findings highlight the importance of surface energy distribution and chemical interactions in the biosorption of MG dye.

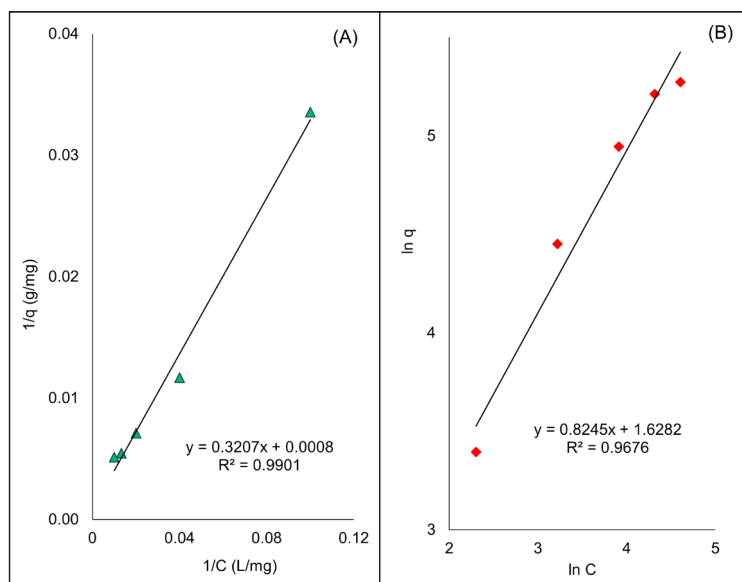


Figure 5. Biosorption isotherms (A) Langmuir and (B) Freundlich of MG onto FeTW

DISCUSSION

MG, a triphenylmethane dye widely used in aquaculture and textile industries, poses substantial health hazards due to its persistence, bioaccumulation, and toxicity. Studies have documented its mutagenic, carcinogenic, and teratogenic effects in both aquatic life and humans upon prolonged exposure (33,34). Thus, the development of low-cost, efficient biosorbents like FeTW that can effectively capture and remove MG from contaminated waters directly supports public health objectives and aligns with SDG 6, 12 and 14.

The FTIR spectral analysis of RTW and FeTW reveals significant alterations in surface functional groups following iron modification, which bear implications for adsorption performance and potential health risk mitigation. Both biosorbents exhibited a broad absorption band around $3,360 \text{ cm}^{-1}$, attributed to O–H stretching vibrations of hydroxyl groups prevalent in lignocellulosic materials. The broader and more intense O–H band in FeTW suggests increased hydrogen bonding capacity, which may enhance dye-biosorbent interactions through polar or electrostatic mechanisms (35,36). This enhanced surface interaction is particularly beneficial for the removal of polar, cationic dyes such as MG.

In both RTW and FeTW, peaks near $2,920 \text{ cm}^{-1}$ correspond to C–H stretching vibrations of aliphatic structures, indicating the preservation of the organic matrix post-modification. Notably, a new absorption peak at approximately $1,730 \text{ cm}^{-1}$ appeared in the FeTW spectrum, corresponding to the C=O stretching vibration. This suggests the formation of carbonyl functionalities during iron impregnation, possibly through oxidative processes, which may serve as active sites for dye molecule complexation via electrostatic or coordinate interactions (37).

The absorption bands near $1,600 \text{ cm}^{-1}$ and $1,400 \text{ cm}^{-1}$, assigned to aromatic C=C and asymmetric/symmetric COO^- stretching, respectively, are consistent with the presence of lignin and hemicellulose-derived structures. These functional groups are known to facilitate dye binding via π – π stacking and ionic interactions. In addition, the C–O and C–O–C stretching vibrations observed between $1,050$ – $1,100 \text{ cm}^{-1}$ further confirm the polysaccharide backbone of the biosorbent, essential for maintaining structural integrity and functional diversity. Crucially, the FeTW spectrum demonstrated a distinct new band around 560 cm^{-1} , corresponding to Fe–O vibrations. The presence of this band confirms the successful incorporation of iron species onto the biosorbent surface.

This structural modification is of particular interest as iron does not only contribute to enhanced adsorption via complexation but may also enable magnetic recovery of the biosorbent, facilitating potential reuse and minimizing secondary waste generation (21,31).

Biosorption was investigated in this study as an environmentally sustainable and economically viable approach for the removal of MG from aqueous solutions. Contact time is a critical operational parameter in biosorption systems, as reducing the time required to reach equilibrium improves treatment efficiency and lowers the potential for prolonged exposure to hazardous pollutants. Rapid removal is particularly important in continuous-flow systems or emergency scenarios, where timely intervention can significantly reduce the risks associated with MG contamination in drinking water sources (38,39). The adsorption behavior of RTW and FeTW exhibited a typical biphasic kinetic profile, characterized by a rapid initial uptake within the first 30 to 45 minutes, followed by a slower phase as equilibrium was approached. Among the two biosorbents, FeTW achieved equilibrium faster, reaching a stable removal capacity within 60 minutes, whereas RTW required approximately 90 minutes. In terms of performance, FeTW demonstrated a higher MG removal efficiency, achieving 38.8%, compared to 34.0% for RTW. The enhanced performance of FeTW can be attributed to a higher density of accessible active sites and the presence of surface functional groups, such as Fe–O and C=O, confirmed through FTIR analysis (21). These modifications likely promote stronger interactions between MG molecules and the biosorbent surface via electrostatic attraction and surface complexation.

The influence of biosorbent dosage was also significant (38,39). FeTW showed a steady increase in removal efficiency as the dosage increased from 0.05 g, which yielded 17.3% removal, to 0.5 g, where the removal efficiency peaked at 68.54%. However, a slight decline in performance was observed at 0.3 g, where the removal efficiency decreased to 36.5%. This reduction is likely due to agglomeration effects that reduce the effective surface area, highlighting the importance of optimizing dosage to ensure maximum dispersion and adsorption capacity. Furthermore, the initial concentration of MG strongly affected biosorption efficiency. When tested with a 25 mg/L solution, FeTW achieved its highest removal efficiency of 68.5%. At higher concentrations, the efficiency declined, with 56.2% removal at 50 mg/L, 48.9% at 75 mg/L, and 39.0% at 100 mg/L. This pattern reflects the saturation of active binding sites as the pollutant load increases, a common limitation in batch adsorption systems (38). These findings underscore the importance of balancing biosorbent mass and contaminant concentration to

maintain effective treatment performance, particularly in industrial wastewater contexts where pollutant levels may fluctuate (38,39).

Isotherm modelling outcomes have significant implications for public health and the environment, as MG is a persistent organic pollutant with documented carcinogenic properties. The Langmuir and Freundlich isotherm models were employed to analyse equilibrium data in order to clarify the biosorption mechanism of MG onto FeTW. The experimental data was well-fitted by the Langmuir model, as evidenced by a high R^2 of 0.9901. This strong agreement suggests that the biosorption process occurred predominantly via monolayer adsorption onto a homogeneous surface with uniform binding energies. The calculated q_m was 45.2 mg/g, demonstrating the high uptake potential of FeTW. Furthermore, the K_L was determined to be 400.88 L/mg, reflecting a strong binding affinity between MG molecules and the FeTW surface. The R_L for an initial MG concentration of 10 mg/L was calculated to be 0.00025, a value well below 1, confirming the highly favorable nature of the biosorption process.

In comparison, the Freundlich model, while slightly less predictive with a R^2 of 0.9676, offered valuable insight into the surface heterogeneity of FeTW with n value in range of 1.21 to 1.45, which is within the accepted range for favorable adsorption, indicating the presence of heterogeneous binding sites and multilayer adsorption. This result complements the Langmuir analysis by suggesting that while monolayer adsorption is dominant, surface heterogeneity also contributes to the biosorption process, enhancing the overall efficiency of MG uptake (29-32). The high adsorption capacity and strong binding affinity demonstrated by FeTW suggest that once MG is adsorbed, it is unlikely to be released back into the environment. Given MG's genotoxicity and capacity for bioaccumulation, the strong FeTW–MG binding interaction reduces environmental mobility and prevents human intake via contaminated water or aquatic organisms, thus lowering public health risks (40-42). This is particularly crucial in preventing prolonged or repeated exposure, which is often associated with chronic health outcomes. The confirmation of monolayer adsorption with strong surface affinity implies that FeTW not only removes MG effectively but also retains it securely, minimizing the risk of secondary contamination.

From a practical standpoint, the ability of FeTW to immobilize MG supports its application in decentralized water treatment systems, particularly in low-resource settings where conventional technologies may be inaccessible. Thus, the isotherm analysis substantiates FeTW as a robust, low-cost, and environmentally

responsible solution for mitigating the toxicological impact of MG in contaminated water sources

ACKNOWLEDGMENTS

The authors gratefully acknowledge Universiti Teknologi MARA, Cawangan Terengganu, Bukit Besi Campus, Dungun, Terengganu, Malaysia and School of Health Sciences, Universiti Sains Malaysia, Health Campus, Kubang Kerian, Kelantan, Malaysia for providing essential support and research facilities.

CONCLUSION

This study demonstrated that FeTW significantly outperforms RTW in MG removal from aqueous solutions with 68.54% removal within 60 minutes at an initial MG concentration of 25mg/L and 0.5 g dosage, compared to 34% by RTW under similar conditions. The enhanced adsorption capacity of FeTW is attributed to improved surface functionality and stronger dye-adsorbent interactions, specifically O–H and Fe–O groups. These findings underscore the practical potential of FeTW as a low-cost, sustainable biosorbent for dye-contaminated wastewater treatment and contribute to reducing public health risks associated with waterborne contaminants. Future work may consider the material's regeneration, stability, and performance in complex wastewater systems to support practical implementation.

AUTHORS' CONTRIBUTION

NHMK: Conceptualization, Methodology, Writing - Original draft preparation. MSNS: Supervision, Writing- Reviewing and Editing, Statistical analysis. NFMS: Software, Validation. AMAZ: Data curation, Writing- Original draft preparation, AAM: Data curation, Writing- Original draft preparation, NARMZ: Software, Validation.

REFERENCES

1. Al-Tohamy R, Ali SS, Li F, Okasha KM, Mahmoud YAG, Elsamahy T, et al. A Critical Review on The Treatment of Dye-Containing Wastewater: Ecotoxicological and Health Concerns of Textile Dyes and Possible Remediation Approaches for Environmental Safety. *Ecotoxicology and Environmental Safety*. 2022;231(113160):1-17. <https://doi.org/10.1016/j.ecoenv.2021.113160>
2. Roy M, Saha R. Dyes and Their Removal Technologies from Wastewater: A Critical Review. In: *Intelligent Environmental Data Monitoring for Pollution Management*. Elsevier eBooks; 2021; 127–160. <https://doi.org/10.1016/b978-0-12-819671-7.00006-3>
3. Nassar S, Sayed AEDH, Allam NN, Ali MM, Mohamed EM. Bioremediation of the Toxic Effects Induced by The Malachite Green Dye in Clarias Gariepinus Using Rhodotorula Mucilaginosa. *Scientific African*. 2024;26(e02496): 1-14. <https://doi.org/10.1016/j.sciaf.2024.e02496>
4. Farhadian S, Hashemi-Shahraki F, Amirifar S, Asadpour S, Shareghi B, Heidari E, et al. Malachite Green, the Hazardous Materials that Can Bind to Apo-Transferrin and Change the Iron Transfer. *International Journal of Biological Macromolecules*. 2022;194:790–799. <https://doi.org/10.1016/j.ijbiomac.2021.11.126>
5. International Agency for Research on Cancer. Malachite Green and Leucomalachite Green. Gentian Violet, Leucogentian Violet, Malachite Green, Leucomalachite Green, and CI Direct Blue 218. *NCBI Bookshelf*, 2022. <https://www.ncbi.nlm.nih.gov/books/NBK594611>
6. Fakhri Y, Mahmoudizheh A, Hemmati F, Adiban M, Esfandiari Z, Mousavi KA. The Concentration of Malachite Green in Fish: A Systematic Review, Meta-Analysis, and Probabilistic Risk Assessment. *International Journal of Environmental Health Research*. 2025;1–16. <https://doi.org/10.1080/09603123.2025.2453971>
7. Khan MD, Singh A, Khan MZ, Tabraiz S, Sheikh J. Current Perspectives, Recent Advancements, and Efficiencies of Various Dye-Containing Wastewater Treatment Technologies. *Journal of Water Process Engineering*. 2023;53(103579): 1-21. <https://doi.org/10.1016/j.jwpe.2023.103579>
8. Fu Z, Chen Z, Yang L, Wang H, Xie J, Ding Z. A RhB@Tb-MOF Sensor for Selective Detection of Malachite Green and Leucomalachite Green. *Journal of Food Composition and Analysis*. 2025;140(107311):1-21. <https://doi.org/10.1016/j.jfca.2025.107311>
9. Abid LH, Mussa ZH, Deyab IF, Al-Ameer LR, Al-Saedi HFS, Al-Qaim FF, et al. Walnut Shell as A Bio-Activated Carbon for Elimination of Malachite Green from its Aqueous Solution: Adsorption Isotherms, Kinetics and Thermodynamic Studies. *Results in Chemistry*. 2025;14(102124):1-10. <https://doi.org/10.1016/j.rechem.2025.102124>
10. Mbuyazi TB, Ajibade PA. Enhanced Photocatalytic Degradation of Malachite Green and Trypan Blue Using 3-Aminopropyl Triethoxysilane (APTES) Functionalized Iron Oxide Nanocomposite. *RSC Advances*. 2025;15(8):6400–6412. <https://doi.org/10.1039/d4ra09025j>
11. Rachma US, Adriyani R, Husnina Z, Farumi SS. Literature Review: Water Quality of Public Bathing, Potential Health Problems and Water Borne Diseases on Visitors. *Jurnal Kesehatan Lingkungan*. 2021;13(2):102-112. <https://doi.org/10.20473/jkl.v13i2.2021.102-112>
12. El HAYA, Hejji L, Seddik NB, Azzouz A, Pérez-Villarejo L, Stitou M, et al. Remediation of Malachite-green Dye from Textile Wastewater Using Biosorbent Almond Shell-based Cellulose. *Journal of Molecular Liquids*. 2024;399(124435):1-11. <https://doi.org/10.1016/j.molliq.2024.124435>
13. Perendija J, Ljubić V, Popović M, Milošević D,

- Arsenijević Z, Đuriš M, et al. Assessment of Waste Hop (*Humulus Lupulus*) Stems as A Biosorbent for The Removal of Malachite Green, Methylene Blue, And Crystal Violet from Aqueous Solution in Batch and Fixed-Bed Column Systems: Biosorption Process and Mechanism. *Journal of Molecular Liquids*. 2023;394(123770):1-19. <https://doi.org/10.1016/j.molliq.2023.123770>
14. Namira KP, Lilis S, Iva REW. Adsorption Kinetics of Banana Stem Activated Carbon in Reducing Phosphate Levels *Jurnal Kesehatan Lingkungan*. 2024;16(1):51–58. <https://doi.org/10.20473/jkl.v16i1.2024.51-58>
 15. Murugesan SR, Sivakumar V, Velusamy S, Ravindiran G, Sundararaj P, Maruthasalam V, et al. Biosorption of Malachite Green from Aqueous Phase by Tamarind Fruit Shells Using FBR. *Advances in Materials Science and Engineering*. 2022; 2022(8565524): 1-7. <https://doi.org/10.1155/2022/8565524>
 16. Christopher JJ, Lydia IS, Sathiyam A, Princy Merlin J. Fabrication of $\text{Cu}_3\text{Mo}_2\text{O}_9$ Doped MWCNT Nanocomposites as Efficient Photocatalyst for Malachite Green Dye Degradation. *Optical Materials*. 2024;156(115935):1-13. <https://doi.org/10.1016/j.optmat.2024.115935>
 17. Mandale P, Kulkarni K, Jadhav K, Kulkarni A, Mahajan R. Adsorption of Malachite Green Dye from Aqueous Solution on Bioadsorbent as Low-Cost Adsorbent. *Materials Today Proceedings*. 2024;1-9 <https://doi.org/10.1016/j.matpr.2024.01.048>
 18. Abbasi F, Mansouri M, Tanzifi M, Ebrahimi F, Sadeghizadeh A. The Modified Pomegranate Peel as An Economical and Highly Effective Adsorbent for Malachite Green Dye Removal from Wastewater. *Colloids and Surfaces C: Environmental Aspects*. 2024;2(100040):1-8. <https://doi.org/10.1016/j.colsuc.2024.100040>
 19. Duarah P, Purkait MK. Fenton Oxidation-Activated Hydrochar Derived from Factory Tea Waste with Enhanced Surface Area as A Sustainable Adsorbent for Multiple Dyes. *Colloids and Surfaces a Physicochemical and Engineering Aspects*. 2025;715(136635):1-15. <https://doi.org/10.1016/j.colsurfa.2025.136635>
 20. Marpongahtun, Andriyani, Muis Y, Gea S, Amaturrehman SA, Attaurrazaq B, et al. Biomass-derived N-doped Carbon Dots/ TiO_2 for Visible-Light-Induced Degradation of Methyl Orange in Wastewater. *Chemistry Africa*. 2024;7(6):3319–3328. <https://doi.org/10.1007/s42250-024-00970-x>
 21. Wu J, Annath H, Chen H, Mangwandi C. Upcycling Tea Waste Particles into Magnetic Adsorbent Materials for Removal of Cr(VI) from Aqueous Solutions. *Particuology*. 2022;80:115–126. <https://doi.org/10.1016/j.partic.2022.11.017>
 22. Abdullah NH, Borhan A, Saadon SHAH. Biosorption of Wastewater Pollutants by Chitosan-based Porous Carbons: A Sustainable Approach for Advanced Wastewater Treatment. *Bioresource Technology Reports*. 2023;25(101705):1-22. <https://doi.org/10.1016/j.biteb.2023.101705>
 23. Khir NHM, Salleh NFM, Ghafar NA, Shukri NM. Mitigating Health Risks Through Biosorption: Effective Removal of Nickel (II) and Chromium (VI) from Water with Acid-Treated Potato Peels *Jurnal Kesehatan Lingkungan*. 2024;16(4):312–320. <https://doi.org/10.20473/jkl.v16i4.2024.312-320>
 24. Debnath S, Das R. Strong Adsorption of CV Dye by Ni Ferrite Nanoparticles for Waste Water Purification: Fits Well the Pseudo Second Order Kinetic and Freundlich Isotherm Model. *Ceramics International*. 2023;49(10): 16199-16215. <https://doi.org/10.1016/j.ceramint.2023.01.218>
 25. Correa-Navarro YM, Rivera-Giraldo JD, Murcia-García JD. Isotherm and Kinetic Data for Adsorption of Butylparaben Onto Biochars Derived from Figue Bagasse. *Data in Brief*. 2024;57(111113):1-8. <https://doi.org/10.1016/j.dib.2024.111113>
 26. Naveen KV, Sathiyaseelan A, Mandal S, Han K, Wang MH. Unveiling the Structural Characteristics and Bioactivities of the Polysaccharides Extracted from Endophytic *Penicillium* sp. *Molecules*. 2023;28(5788):1-19. <https://doi.org/10.3390/molecules28155788>
 27. Liu X, Renard CMGC, Bureau S, Le Bourvellec C. Revisiting the Contribution of ATR-FTIR Spectroscopy to Characterize Plant Cell Wall Polysaccharides. *Carbohydrate Polymers*. 2021;262(117935):1-10. <https://doi.org/10.1016/j.carbpol.2021.117935>
 28. Selvaraj R, Murugesan G, Rangasamy G, Bhole R, Dave N, Pai S, et al. As (III) Removal Using Superparamagnetic Magnetite Nanoparticles Synthesized Using *Ulva Prolifera* – optimization, Isotherm, Kinetic and Equilibrium Studies. *Chemosphere*. 2022;308(136271):1-12. <https://doi.org/10.1016/j.chemosphere.2022.136271>
 29. Alabi AH, Akano OR, Ekele WK, Olanrewaju CA, Oladaye PO, Obayomi KS. Biosorptive Removal of Toxic Nitrate Ion from Wastewater Using Albizia Lebbeck Seed Pods: Isotherm and Equilibrium Studies. *Journal of the Indian Chemical Society*. 2024;101(101353):1-10. <https://doi.org/10.1016/j.jics.2024.101353>
 30. Cao W, Wu D, Xiao P. Synthesis of Chitosan-Glutaraldehyde/Activated Carbon Composite for Methylene Blue Adsorption: Optimization and Mechanisms. *Desalination and Water Treatment*. 2022;270:275–288. <https://doi.org/10.5004/dwt.2022.28793>
 31. Wang J, Huang X, Chen Z, Chen N, Yang M, Liang C, et al. Extraction and Purification of Total Flavonoids from *Zanthoxylum Planispinum* Var. *Dintanensis* Leaves and Effect of Altitude on Total Flavonoids Content. *Scientific Reports*. 2025;15(1):1-15. <https://doi.org/10.1038/s41598-025-91528-5>
 32. Hajiaghbababaei L, Mazloomifar A, Khalilian F, Farahani GT. Functionalization Of Magnetic Nanoparticles with 1-cyclopropyl-6-fluoro-4-oxo-7-(piperazin-1-yl)-1,4-dihydroquinoline-3-carboxylic acid As an Efficient Adsorbent for The Gefitinib Removal from Water. *Scientific Reports*. 2025;15(5905):1-15. <https://doi.org/10.1038/s41598-025-89641-6>
 33. Poopal RK, Ashwini R, Ramesh M, Li B, Ren Z.

- Triphenylmethane Dye ($C_{52}H_{54}N_4O_{12}$) is Potentially a Hazardous Substance in Edible Freshwater Fish at Trace Level: Toxicity, Hematology, Biochemistry, Antioxidants, and Molecular Docking Evaluation Study. *Environmental Science and Pollution Research*. 2022;30(11):28759–28779. <https://doi.org/10.1007/s11356-022-24206-y>
34. Himanshu, Behera B, Kumari N, Maruthi M, Singh RK, Saini JK. Appraisal Of Malachite Green Biodegradation and Detoxification Potential of Laccase from *Trametes Cubensis*. *Bioresource Technology*. 2024;417(131869):1-10. <https://doi.org/10.1016/j.biortech.2024.131869>
 35. Ahmad A, Jamil SNAMd, Choong TSY, Abdullah AH, Faujan NH, Adeyi AA, et al. Removal of Cationic Dyes by Iron Modified Silica/Polyurethane Composite: Kinetic, Isotherm and Thermodynamic Analyses, and Regeneration Via Advanced Oxidation Process. *Polymers*. 2022;14(5416):1-23. <https://doi.org/10.3390/polym14245416>
 36. Md Salim R, Asik J, Sarjadi MS. Chemical Functional Groups of Extractives, Cellulose and Lignin Extracted from Native *Leucaena Leucocephala* Bark. *Wood Science and Technology*. 2021;55(2):295–313. <https://doi.org/10.1007/s00226-020-01258-2>
 37. Gong M, Xu F, Liu P, Xu Q, Su Y, Fan Y, et al. A review of biomass hydrochar as an adsorbent: Performance, modification, and applications. *Journal of Water Process Engineering*. 2025;71(107314):1-20. <https://doi.org/10.1016/j.jwpe.2025.107314>
 38. Kali A, Dehmani Y, Amar A, Loulidi I, El-kordy A, Jabri M, et al. Almond Shells Based-lignocellulosic Waste Materials for A High Removal Efficacy of Chromium (VI) Ions from Waste Water. *Interactions*. 2025;246(1):1-20. <https://doi.org/10.1007/s10751-025-02264-1>
 39. Alzura SP, Saraswat V, Ishmayana S, Budiman YP, Eddy DR, Aji ES, et al. Synthesis and Characterization of Zinc Oxide Nanoparticles-carbon Composite Derived from Pineapple Peel Wastes for Adsorption of Methylene Blue from Solution and Photocatalytic Activity. *Case Studies in Chemical and Environmental Engineering*. 2025;11(101113):1-10. <https://doi.org/10.1016/j.cscee.2025.101113>
 40. Abdul Aziz A, Osman MS, Wan Rasdi N, Shafie FA, Feisal NAS, Zaki MA, et al. Assessing Microplastic Contamination in Shellfish: Insights from Pantai Remis Kuala Selangor, Strait of Malacca, Malaysia. *Jurnal Kesehatan Lingkungan*. 2024;16(4):321–330. <https://doi.org/10.20473/jkl.v16i4.2024.321-330>
 41. Ibrahim TNB, Jesi AA, Feisal NAS, Windusari Y, Samat NA, Kamaludin NH, et al. Klang River Water Quality Assessment and its Effects on Human Health Using Chemometric Analysis. *Jurnal Kesehatan Lingkungan*. 2024;16(2):125–136. <https://doi.org/10.20473/jkl.v16i2.2024.125-136>
 42. Esumeh CO, Andrew R. Incidence of Pathogens in Fruits and Vegetables in Tropical Bwari Town. *Jurnal Kesehatan Lingkungan*. 2024;16(4):342–350. <https://doi.org/10.20473/jkl.v16i4.2024.342-350>